Automatica 93 (2018) 244–256

Contents lists available at ScienceDirect

Automatica

journal homepage: www.elsevier.com/locate/automatica

A decentralized energy-optimal control framework for connected automated vehicles at signal-free intersections☆

Andreas A. Malikopoulos [a,*], Christos G. Cassandras [b], Yue J. Zhang [b]

[a] Department of Mechanical Engineering, University of Delaware, 126 Spencer Lab, 130 Academy Street, Newark, DE, 19716, USA
[b] Division of Systems Engineering and Center for Information and Systems Engineering, Boston University, 15 Saint Mary's Street, Brookline, MA, 02446, USA

ARTICLE INFO

Article history:
Received 30 April 2017
Received in revised form 17 January 2018
Accepted 25 February 2018
Available online 31 March 2018

Keywords:
Connected and automated vehicles
Decentralized optimal control
Autonomous intersections
Traffic flow
Motion planning
Energy usage
Safety

ABSTRACT

We address the problem of optimally controlling connected and automated vehicles (CAVs) crossing an urban intersection without any explicit traffic signaling, so as to minimize energy consumption subject to a throughput maximization requirement. We show that the solution of the throughput maximization problem depends only on the hard safety constraints imposed on CAVs and its structure enables a decentralized optimal control problem formulation for energy minimization. We present a complete analytical solution of these decentralized problems and derive conditions under which feasible solutions satisfying all safety constraints always exist. The effectiveness of the proposed solution is illustrated through simulation which shows substantial dual benefits of the proposed decentralized framework by allowing CAVs to conserve momentum and fuel while also improving travel time.

1. Introduction

Next generation transportation networks are typical cyber–physical systems where event-driven components monitor and control physical entities online. We are currently witnessing an increasing integration of energy, transportation, and cyber networks, which, coupled with human interactions, is giving rise to a new level of complexity in the transportation network and necessitates new control and optimization approaches.

The alarming state of current transportation systems is well documented. In 2014, congestion caused vehicles in urban areas to spend 6.9 billion additional hours on the road at a cost of an extra 3.1 billion gallons of fuel, resulting in a total cost estimated at $160 billion; see Schrank, Eisele, Lomax, and Bak (2015). From a control and optimization standpoint, the challenge is to develop mechanisms that expand capacity *without* affecting the existing road infrastructure, specifically by tighter spacing of vehicles in roadways and better control at the weakest links of a transportation system: the bottleneck points defined by intersections, merging roadways, and speed reduction zones; see Malikopoulos and Aguilar (2013) and Margiotta and Snyder (2011). An automated highway system (AHS) can alleviate congestion, reduce energy use and emissions, and improve safety by significantly increasing traffic flow as a result of closer packing of automatically controlled vehicles. Forming "platoons" of vehicles traveling at high speed is a popular system-level approach to address traffic congestion that gained momentum in the 1990s; see Rajamani, Tan, Law, and Zhang (2000) and Shladover et al. (1991). More recently, a study in Tachet et al. (2016) indicated that transitioning from intersections with traffic lights to autonomous ones has the potential of doubling capacity and reducing delays.

Connected and automated vehicles (CAVs) provide the most intriguing opportunity for enabling users to better monitor transportation network conditions and to improve traffic flow. CAVs can be controlled at different transportation segments, e.g., intersections, merging roadways, roundabouts, speed reduction zones and can assist drivers in making better operating decisions to improve safety and reduce pollution, energy consumption, and travel delays. One of the very early efforts in this direction was proposed in Athans (1969) and Levine and Athans (1966) where the merging problem was formulated as a linear optimal regulator to control a single string of vehicles. Varaiya (1993) has also discussed

☆ This research was supported by the US Department of Energy's (DOE) SMART Mobility Initiative. The work of Cassandras and Zhang is supported in part by NSF under grants CNS-1239021, ECCS-1509084, CNS-1645681, and IIP-1430145, by AFOSR under grant FA9550-15-1-0471, by The MathWorks and by Bosch. The material in this paper was partially presented at the 2016 American Control Conference, July 68, 2016, Boston, MA, USA. This paper was recommended for publication in revised form by Associate Editor Richard D. Braatz under the direction of Editor Thomas Parisini.

* Corresponding author.
E-mail addresses: andreas@udel.edu (A.A. Malikopoulos), cgc@bu.edu (C.G. Cassandras), joycez@bu.edu (Y.J. Zhang).

https://doi.org/10.1016/j.automatica.2018.03.056
0005-1098/

extensively the key features of an automated intelligent vehicle-highway system (IVHS) and proposed a related control system architecture.

In this paper, we address the problem of optimally controlling CAVs crossing an urban intersection without any explicit traffic signaling so as to minimize energy consumption subject to a throughput maximization requirement and to hard safety constraints. The implications of this approach are that vehicles do not have to come to a full stop at the intersection, thereby conserving momentum and fuel while also improving travel time. Moreover, by optimizing each vehicle's acceleration/deceleration, we minimize transient engine operation, thus we have additional benefits in fuel consumption. Several research efforts have been reported in the literature proposing either *centralized* (if there is at least one task in the system that is globally decided for all vehicles by a single central controller) or *decentralized* approaches for coordinating CAVs at intersections. Dresner and Stone (2004) proposed the use of a centralized reservation scheme to control a single intersection of two roads with no turns allowed. Since then, numerous centralized approaches have been reported in the literature, e.g., de La Fortelle (2010), Dresner and Stone (2008) and Huang, Sadek, and Zhao (2012), to achieve safe and efficient control of traffic through intersections. Some approaches have focused on coordinating vehicles to improve the travel time, e.g., Yan, Dridi, and El Moudni (2009), Zhu and Ukkusuri (2015) and Zohdy, Kamalanathsharma, and Rakha (2012). Others have considered minimizing the overlap in the position of vehicles inside the intersection rather than arrival time; see Lee, Park, Malakorn, and So (2013). Kim and Kumar (2014) proposed an approach based on model predictive control that allows each vehicle to optimize its movement locally with respect to any objective of interest. Miculescu and Karaman (2014) used queueing theory and modeled the problem as a polling system that determines the sequence of times assigned to the vehicles on each road.

In decentralized approaches, each vehicle determines its own control policy based on the information received from other vehicles on the road or from a coordinator. Alonso et al. (2011) proposed two conflict resolution schemes in which an autonomous vehicle can make a decision about the appropriate order of crossing the intersection to avoid collision with other manually driven vehicles. Colombo and Del Vecchio (2014) constructed the invariant set for the control inputs that ensure lateral collision avoidance. A detailed discussion of research efforts in this area can be found in Rios-Torres and Malikopoulos (2017a).

The first contribution of the paper is the formulation of an energy minimization optimal control problem for CAVs where the time for each CAV to cross the intersection is first determined as the solution of a throughput maximization problem. We show that the solution structure of the latter problem enables a decentralized energy minimization optimal control problem formulation whose terminal time depends only on a "neighboring" CAV set. An analytical solution of each CAV's optimal control problem without considering state and control constraints was presented in Ntousakis, Nikolos, and Papageorgiou (2016), Rios-Torres and Malikopoulos (2017b) and Rios-Torres, Malikopoulos, and Pisu (2015) for CAVs at highway on-ramps, and in Zhang, Malikopoulos, and Cassandras (2016) for two adjacent intersections. Unlike all these prior formulations, we specify the explicit connection between the energy minimization and throughput maximization problems, do not impose constraints on the terminal CAV speeds, and present a complete analytical solution that includes all state and control constraints. Ensuring that a *feasible* solution to each CAV decentralized optimal control problem exists is nontrivial, as discussed in Zhang, Cassandras, and Malikopoulos (2017). Thus, another contribution is showing that this solution depends on the arrival time of a CAV at a "control zone" defined for the intersection and on its initial speed and then providing a proof (not given in Zhang, Cassandras et al. (2017)) of the existence of a nonempty feasibility region in the space defined by this arrival time and initial speed.

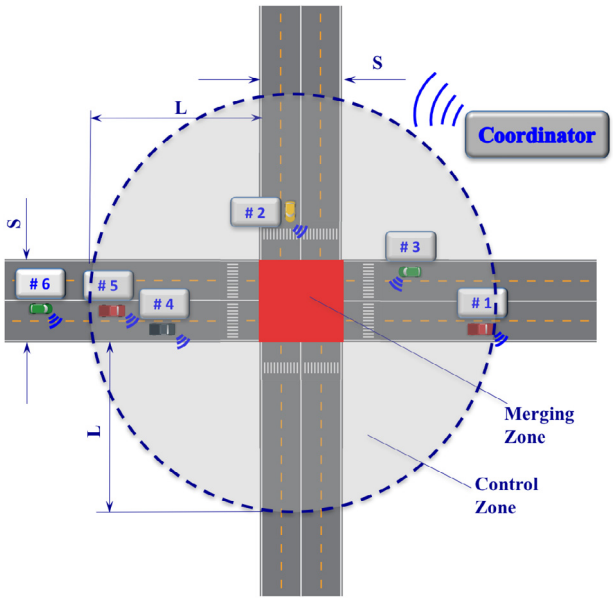

Fig. 1. Intersection with connected and automated vehicles.

The paper is organized as follows. In Section 2, we introduce the modeling framework, formulate the energy-minimization optimal control problem and establish its connection to throughput maximization. In Section 3, we present the decentralized control framework, derive a closed-form analytical solution for each decentralized problem, and show the existence of feasible solutions ensuring that all safety constraints remain inactive. Finally, we provide simulation results in Section 4 illustrating the effectiveness of the proposed solution in terms of significant reductions in both fuel consumption and travel time. Concluding remarks are given in Section 5.

2. Problem formulation

We consider an intersection (Fig. 1) where the region at its center is called *Merging Zone* (MZ) and is the area of potential lateral collision of vehicles. Although this is not restrictive, we consider the MZ to be a square of side S. The intersection has a *Control Zone* (CZ) and a coordinator that can communicate with the vehicles traveling inside the CZ. Note that the coordinator is not involved in any decision for any CAV and only enables communication of appropriate information among CAVs. The distance from the entry of the CZ to the entry of the MZ is L and it is assumed to be the same for all CZ entry points. The value of L depends on the coordinator's communication range capability with the CAVs, while S is the physical length of a typical intersection. In this paper, we limit ourselves to the case of no lane changes and no turns allowed.

Let $N(t) \in \mathbb{N}$ be the number of CAVs inside the CZ at time $t \in \mathbb{R}^+$ and $\mathcal{N}(t) = \{1, \ldots, N(t)\}$ be a queue which designates the order in which these vehicles will be entering the MZ. Thus, letting t_i^m be the assigned time for vehicle i to enter the MZ, we require that

$$t_i^m \geq t_{i-1}^m, \ \forall i \in \mathcal{N}(t), \ i > 1. \tag{1}$$

There is a number of ways to satisfy (1). For example, we may impose a strict first-in-first-out queueing structure, where each vehicle must enter the MZ in the same order it entered the CZ. More

generally, however, t_i^m may be determined for each vehicle i at time t_i^0 when the vehicle enters the CZ and $\mathcal{N}(t_i^0) = \{1, \ldots, i-1\}$. If $t_i^m > t_{i-1}^m$, then the order in the queue is preserved. If, on the other hand, there exists some $j \in \mathcal{N}(t_i^0)$, where $j < i-1$, such that $t_j^m > t_i^m > t_{j-1}^m$, then the order is updated so that CAV i is placed in the jth queue position. The policy through which the order ("schedule") is specified may be the result of a higher level optimization problem as long as the condition $t_i^m \geq t_{i-1}^m$ is preserved in between CAV arrival events at the CZ. In what follows, we will adopt a specific scheme for determining t_i^m (upon arrival of CAV i) based on our problem formulation, without affecting $t_1^m, \ldots, t_{i-1}^m$, but we emphasize that our analysis is not restricted by the policy designating the order of the vehicles within the queue $\mathcal{N}(t)$.

2.1. Vehicle model, constraints, and assumptions

For simplicity, we represent the dynamics of each CAV $i \in \mathcal{N}(t)$, moving along a specified lane through second order dynamics

$$\begin{aligned} \dot{p}_i &= v_i(t), \quad p_i(t_i^0) = 0 \\ \dot{v}_i &= u_i(t), \quad v_i(t_i^0) \text{ given} \end{aligned} \tag{2}$$

where t_i^0 is the time when CAV i enters the CZ, and $p_i(t) \in \mathcal{P}_i$, $v_i(t) \in \mathcal{V}_i$, $u_i(t) \in \mathcal{U}_i$ denote the position, speed and acceleration/deceleration (control input) of each CAV i inside the CZ. The sets $\mathcal{P}_i$, $\mathcal{V}_i$ and $\mathcal{U}_i$, $i \in \mathcal{N}(t)$, are complete and totally bounded subsets of $\mathbb{R}$. The state space $\mathcal{P}_i \times \mathcal{V}_i$ is closed with respect to the induced topology, thus, it is compact.

We need to ensure that for any initial time and state (t_i^0, p_i^0, v_i^0) and every admissible control $u(t)$, the system (2) has a unique solution $(p_i(t), v_i(t))$ on some interval $[t_i^0, t_i^m]$, where t_i^m is the time that vehicle $i \in \mathcal{N}(t)$ enters the MZ. To ensure that the control input and vehicle speed are within a given admissible range, the following constraints are imposed:

$$\begin{aligned} &u_{i,min} \leqslant u_i(t) \leqslant u_{i,max}, \quad \text{and} \\ &\quad 0 \leqslant v_{min} \leqslant v_i(t) \leqslant v_{max}, \quad \forall t \in [t_i^0, t_i^m], \end{aligned} \tag{3}$$

where $u_{i,min}$, $u_{i,max}$ are the minimum and maximum control inputs (maximum deceleration/acceleration) for each vehicle $i \in \mathcal{N}(t)$, and v_{min}, v_{max} are the minimum and maximum speed limits respectively. For simplicity, in the sequel we do not consider vehicle diversity and thus set $u_{i,min} = u_{min}$ and $u_{i,max} = u_{max}$.

Definition 1. Depending on its physical location inside the CZ, CAV $i-1 \in \mathcal{N}(t)$ belongs to only one of the following four subsets of $\mathcal{N}(t)$ with respect to CAV i: (1) $\mathcal{R}_i(t)$ contains all CAVs traveling on the same road as i and towards the same direction but on different lanes (e.g., $\mathcal{R}_6(t)$ contains CAV 4 in Fig. 1), (2) $\mathcal{L}_i(t)$ contains all CAVs traveling on the same road and lane as vehicle i (e.g., $\mathcal{L}_6(t)$ contains CAV 5 in Fig. 1), (3) $\mathcal{C}_i(t)$ contains all CAVs traveling on different roads from i and having destinations that can cause collision at the MZ, (e.g., $\mathcal{C}_6(t)$ contains CAV 2 in Fig. 1), and (4) $\mathcal{O}_i(t)$ contains all CAVs traveling on the same road as i and opposite destinations that cannot, however, cause collision at the MZ (e.g., $\mathcal{O}_6(t)$ contains CAV 3 in Fig. 1).

Based on this definition, it is clear that a rear-end collision can only arise if CAV $k \in \mathcal{L}_i(t)$ is directly ahead of i. Thus, to ensure the absence of any rear-end collision, we assume a predefined safe distance $\delta < S$ and impose the rear-end safety constraint

$$s_i(t) = p_k(t) - p_i(t) \geqslant \delta, \ \forall t \in [t_i^0, t_i^f], k \in \mathcal{L}_i(t) \tag{4}$$

where t_i^f is the time that CAV $i \in \mathcal{N}(t)$ exits the MZ. The rear-end safety constraint is usually expressed in terms of the allowable headway (Rajamani, 2012), i.e., a time gap that is a function of speed. However, since we consider urban intersections, the average speed does not exhibit significant variations. Therefore, we can translate the allowable headway to a safe inter-vehicle distance. In the rest of the paper, we reserve the symbol k to denote the CAV which is physically immediately ahead of i in the same lane.

A lateral collision involving CAV i may occur only if some CAV $j \neq i$ belongs to $\mathcal{C}_i(t)$. This leads to the following definition:

Definition 2. For each CAV $i \in \mathcal{N}(t)$, we define the set Γ_i that includes all time instants when a lateral collision involving CAV i is possible:

$$\Gamma_i \triangleq \left\{ t \mid t \in [t_i^m, t_i^f] \right\}. \tag{5}$$

Consequently, to avoid a lateral collision for any two vehicles $i, j \in \mathcal{N}(t)$ on different roads, the following constraint should hold

$$\Gamma_i \cap \Gamma_j = \varnothing, \quad \forall t \in [t_i^m, t_i^f], j \in \mathcal{C}_i(t). \tag{6}$$

This constraint implies that no two CAVs from different roads which may lead to a lateral collision are allowed to be in the MZ at the same time. If the length of the MZ is large, then this constraint might not be realistic, but it can be modified appropriately as described in Remark 2.

In the modeling framework described above, we impose the following assumptions:

Assumption 1. For CAV i, none of the constraints (3)–(4) is active at t_i^0.

Assumption 2. The speed of the CAVs inside the MZ is constant, i.e., $v_i(t) = v_i(t_i^m) = v_i(t_i^f)$, $\forall t \in [t_i^m, t_i^f]$ This implies that

$$t_i^f = t_i^m + \frac{S}{v_i(t_i^m)}. \tag{7}$$

Assumption 3. Each CAV i has proximity sensors and can measure local information without errors or delays.

Assumption 1 ensures that the initial state and control input are feasible. Enforcing this is nontrivial and we address the issue in Section 3.2. The second assumption is intended to enhance safety awareness, but it could be modified appropriately, if necessary, as discussed in Section 2.2. The third assumption may be strong, but it is relatively straightforward to relax as long as the noise in the measurements and/or delays is bounded. For example, we can determine upper bounds on the state uncertainties as a result of sensing or communication errors and delays, and incorporate these into more conservative safety constraints.

For simplicity of notation in the remainder of the paper, we will write $v_i(t_i^0) \equiv v_i^0$, $v_i(t_i^m) \equiv v_i^m$ and $v_i(t_i^f) \equiv v_i^f$.

2.2. Energy minimization problem formulation

We begin by considering the controllable acceleration/deceleration $u_i(t)$ of each CAV i which minimizes the following cost functional:

$$J_i(u_i(t), t_i^m) = \int_{t_i^0}^{t_i^m} C_i(u_i(t))dt, \tag{8}$$

$$\text{subject to : (2), (3), (4), (6), } \quad p_i(t_i^0) = 0, p_i(t_i^m) = L,$$

$$\text{and given } t_i^0, v_i^0, t_i^m.$$

We view $C_i(u_i(t))$ as a measure of the energy, which is a function of the control input (acceleration/deceleration) consumed by CAV i in traveling between $p_i(t_i^0) = 0$ and $p_i(t_i^m) = L$; see Malikopoulos (2011). A special case arises when the cost function is the L^2-norm

of the control input in $[t_i^0, t_i^m]$ and $C_i(u_i(t)) = \frac{1}{2}u_i^2(t)$. In this case, we minimize transient engine operation, thus we can have direct benefits in fuel consumption and emissions since internal combustion engines are optimized over steady state operating points (constant torque and speed); see Malikopoulos (2013) and Rios-Torres and Malikopoulos (2017b). In this problem, t_i^0, v_i^0 are known upon arrival of CAV i at the CZ and t_i^m is also specified. Clearly, not all t_i^m can satisfy the safety constraints (4) and (6). Moreover, in general, a value of t_i^m that satisfies (4) and (6) may depend on other CAVs $j \neq i$; therefore, it may not be possible for CAV i to solve (8) in a *decentralized* manner, i.e., based only on local information. We address the question of specifying appropriate t_i^m for each instance of (8) in what follows.

Before proceeding, we note that the obvious unconstrained solution to (8) is $u_i^*(t) = 0$ for all $t \in [t_i^0, t_i^m]$. This applies to $i = 1$ since, in this case, (4) and (6) are inactive, since it is not constrained by any prior CAV in the queue, and t_1^m variable. This also implies that $v_1^*(t) = v_i^0$ for all $t \in [t_i^0, t_i^m]$ and $t_1^m = L/v_i^0$.

We now turn our attention to the problem of maximizing the traffic throughput at the intersection, in terms of minimizing the gaps between the vehicles in a given queue $\mathcal{N}(t)$ (see Fig. 1), under the hard safety constraints (4) and (6). Thus, setting $\mathbf{t}_{(2:N(t))} = [t_2^m \dots t_{N(t)}^m]$, we define the following optimization problem:

$$\min_{\mathbf{t}_{(2:N(t))}} \sum_{i=2}^{N(t)} \left(t_i^m - t_{i-1}^m\right) = \min_{\mathbf{t}_{N(t)}} \left(t_{N(t)}^m - t_1^m\right), \tag{9}$$

subject to : (1), (3), (4), (6)

where t_1^m is not included since it is obtained from the solution of (8) when $i = 1$, i.e., $t_1^m = L/v_i^0$. The equivalence between the two expressions in (9) (due to the cancellation of all terms in the sum except the first and last) reflects the equivalence between minimizing the total time to process all CAVs in the queue and the average interarrival time of CAVs at the MZ.

As stated in (9), the problem does not incorporate constraints on t_i^m, $i = 2, \dots, N(t)$, that are imposed by the CAV dynamics. In other words, we should write $t_i^m = t_i^m(\mathbf{u}_{(1:i)}(t))$ where $\mathbf{u}_{(1:i)}(t) = [u_1(t; t_1^m) \dots u_i(t; t_i^m)]$ denotes the controls applied to all CAVs $i = 1, \dots, N(t)$ over $[t_i^0, t_i^m]$ for any given t_i^0, t_i^m. Let $\mathscr{A}_i$ denote a set of feasible controls:

$$\mathscr{A}_i \triangleq \Big\{ u_i(t; t_i^m) \in \mathcal{U}_i \text{ subject to:} \tag{10}$$
$$(1), (2), (3), (4), (6),\ p_i(t_i^0) = 0, p_i(t_i^m) = L,$$
$$\text{and given } t_i^0, v_i^0, t_i^m \Big\}.$$

Then, we rewrite (9) as

$$\min_{\mathbf{t}_{(2:N(t))}} \sum_{i=2}^{N(t)} \left(t_i^m(\mathbf{u}_{(1:i)}(t)) - t_{i-1}^m(\mathbf{u}_{(1:i-1)}(t))\right) \tag{11}$$
$$= \min_{\mathbf{t}_{N(t)}} \left(t_{N(t)}^m(\mathbf{u}_{(1:N(t))}(t)) - t_1^m(\mathbf{u}_{(1)}(t))\right),$$

subject to : $u_i(t; t_i^m) \in \mathscr{A}_i,\ \forall i \in \mathcal{N}(t),\ (1),\ (3),\ (4),\ (6).$

Remark 1. As pointed out earlier, the solution of (8) for $i = 1$ is $u_1^*(t) = 0$ resulting in $v_1^*(t) = v_i^0$ and $t_1^{m*} = L/v_i^0$. On the other hand, if we were to solve (11) for $i = 1$ setting $t_0^m = 0$, the solution would be $t_1^{m*} = t_1^m = L/v_{max}$. This indicates a degree of freedom in the selection of t_1^m which can be used to trade off the energy minimization and throughput maximization (congestion reduction) objectives. Thus, t_1^m may be viewed as a parameter one can adjust to solve the subsequent CAV problems placing a desired amount of emphasis on throughput relative to energy consumption.

The solution of (11) provides a sequence $\{t_2^{m*}, \dots, t_{N(t)}^{m*}\}$ which designates the MZ arrival times of all CAVs in the current queue so as to minimize the total time needed for them to clear the intersection (recalling Assumption 2, the time through the MZ is fixed), hence maximizing the throughput over the current $N(t)$ CAVs. This solution may then be used in (8) to specify the terminal time of each energy minimization problem. In what follows, we show that this solution has a simple iterative structure and depends only on the hard safety constraints (4) and (6), as well as the state and control constraints (3). We begin by ignoring the latter to obtain the following result.

Lemma 1. *Suppose that the constraints (3) are inactive in (11). Then, the solution $\mathbf{t}^* = [t_2^{m^*}, \dots, t_N^{m^*}]$ of problem (11) is determined through the following recursive structure over $i = 2, \dots, N$:*

$$t_i^{m^*} = \begin{cases} \max\{t_{i-1}^{m^*}, t_k^{m^*} + \dfrac{\delta}{v_k^m}\} & \text{if } i-1 \in \mathcal{R}_i(t) \cup \mathcal{O}_i(t) \\ t_{i-1}^{m^*} + \dfrac{\delta}{v_{i-1}^m} & \text{if } i-1 \in \mathcal{L}_i \\ t_{i-1}^{m^*} + \dfrac{S}{v_{i-1}^m} & \text{if } i-1 \in \mathcal{C}_i \end{cases} \tag{12}$$

where $k = \max\{j : j \in \mathcal{L}_i(t), j = 1, \dots, i-2\} < i$ is the CAV which is physically immediately ahead of i in the same lane.

Proof. See Appendix.

Remark 2. The lateral collision constraint (6) allows only one CAV at a time to be inside the MZ. If the length of the MZ is large, however, then this constraint may become overly conservative, since it results in dissipating space and road capacity. The constraint can be modified appropriately and (52) in *Case 3* above can be rewritten as

$$t_i^{m^*} = t_{i-1}^{m^*} + \frac{r}{v_{i-1}^m} \tag{13}$$

with any desired distance $r < S$ between CAVs inside the MZ.

Next, we relax the assumption made in Lemma 1 that constraints (3) are inactive in (11) and derive a recursive equation for the determination of $\mathbf{t}^* = [t_2^{m^*}, \dots, t_N^{m^*}]$.

Theorem 1. *The solution $\mathbf{t}^* = [t_1^{m^*}, \dots, t_N^{m^*}]$ of problem (11) is recursively determined through*

$$t_i^{m^*} = \begin{cases} t_1^{m^*} & \text{if } i = 1 \\ \max\{t_{i-1}^{m^*}, t_k^{m^*} + \dfrac{\delta}{v_k^m}, t_i^c\} & \text{if } i-1 \in \mathcal{R}_i(t) \cup \mathcal{O}_i(t) \\ \max\{t_{i-1}^{m^*} + \dfrac{\delta}{v_{i-1}^m}, t_i^c\} & \text{if } i-1 \in \mathcal{L}_i \\ \max\{t_{i-1}^{m^*} + \dfrac{S}{v_{i-1}^m}, t_i^c\} & \text{if } i-1 \in \mathcal{C}_i \end{cases} \tag{14}$$

where $t_i^c = t_i^1 \mathbb{1}_{v_i^m = v_{max}} + t_i^2(1 - \mathbb{1}_{v_i^m = v_{max}})$ and

$$t_i^1 = t_i^0 + \frac{L}{v_{max}} + \frac{(v_{max} - v_i^0)^2}{2u_{i,max}v_{max}} \tag{15}$$

$$t_i^2 = t_i^0 + \frac{[2Lu_{i,max} + (v_i^0)^2]^{1/2} - v_i^0}{u_{i,max}}. \tag{16}$$

Proof. See Appendix.

It follows from Theorem 1 that $t_i^{m^*}$ is always recursively determined from $t_{i-1}^{m^*}$ and v_{i-1}^m and possibly $t_k^{m^*}$, v_k^m where v_{i-1}^m and v_k^m depend on the specific controls used when solving problem (11).

However, note that there is no guarantee that there exist feasible controls satisfying all constraints in (10) over all $t \in [t_i^0, t_i^m]$. In fact, as we will discuss in Section 3.2, it is easy to see that the safety constraint (4) may not hold depending on the initial conditions (t_i^0, v_i^0) for CAV i. We will show, however, in Theorem 2 that there exists a nonempty feasible region $\mathcal{F}_i \subset R^2$ of initial conditions (t_i^0, v_i^0) such that $s_i(t) \geqslant \delta$ for all $t \in (t_i^0, t_i^m)$ so that all safety constraints are guaranteed to hold throughout $[t_i^0, t_i^m]$.

We are now in a position to return to the energy minimization problem (8) with the value of t_i^m for any $i = 1, \ldots, N(t)$ specified through (14) in a recursive manner. This allows us to solve these problems in a decentralized manner as detailed in the next section.

3. Decentralized framework

The results in the previous section allow us to address the optimal control problem (8) within a decentralized framework. However, to establish this framework, we need a communication structure between CAVs with a "coordinator" whose task is to handle the information between them. In particular, when a CAV i reaches the CZ of the intersection at some instant t, the coordinator assigns to it a unique identity as follows.

Let $M(t) \in \mathbb{N}$ be the cumulative number of CAVs that have entered the CZ by time t. Note that $M(t)$ is increasing in t and can be reset to $M(t) = 0$ only if no CAVs are inside the CZ. The *unique identity* that the coordinator assigns to each CAV is a triplet (w, i, j) where $w = M(t) + 1$ is a unique index, i is the position of the vehicle in the current queue $\mathcal{N}(t)$, and $j \in \{1, \ldots, 4\}$ is an integer based on a one-to-one mapping from $\{\mathcal{R}_i(t), \mathcal{L}_i(t), \mathcal{C}_i(t), \mathcal{O}_i(t)\}$ onto $\{1, \ldots, 4\}$ that indicates the positional relationship between CAVs $i-1$ and i. If two or more CAVs enter the CZ at the same time, then the coordinator assigns randomly the index w.

Definition 3. For each vehicle i entering a CZ, we define the *information set* $Y_i(t)$ as

$$Y_i(t) \triangleq \left\{p_i(t), v_i(t), w, \mathcal{Q}_i, s_i(t), t_i^{m^*}\right\}, \forall t \in [t_i^0, t_i^{m^*}], \tag{17}$$

where $p_i(t), v_i(t)$ are the position and speed of CAV i inside the CZ; w and $\mathcal{Q}_i \in \{1, \ldots, 4\}$ are the unique index and the queue subset (Definition 1) assigned to CAV i by the coordinator; and $s_i(t) = p_k(t) - p_i(t)$ is the distance between CAV i and some CAV k which is immediately ahead of i in the same lane (recall that we reserve the symbol k to denote such a CAV relative to i). The last element above, $t_i^{m^*}$, is the time targeted for CAV i to enter the MZ and is given in (14) depending on the value of $\mathcal{Q}_i$.

Note that once CAV i enters the CZ, then immediately all information in $Y_i(t)$ becomes available to i: $p_i(t), v_i(t)$ are read from its sensors; $\mathcal{Q}_i$ is assigned by the coordinator, as is the value of k based on which $s_i(t)$ is also evaluated; $t_i^{m^*}$ can also be computed at that time based on the information the vehicle i receives from $i-1$. The recursion on $t_i^{m^*}$ is initialized whenever a vehicle enters the CZ. In this case, t_1^m can be externally assigned as the desired exit time of this vehicle whose behavior is unconstrained (as discussed in the previous section). Thus, the time t_1^m is available through $Y_1(t)$.

Since the coordinator is not involved in any control decision, from Theorem 1 we can formulate $N(t)$ sequential decentralized tractable problems of the form (8) that may be solved online. As already discussed, a special case of (8) arises when the cost function is the L^2-norm of the control input in $[t_i^0, t_i^{m^*}]$ which we shall henceforth consider. Thus, the decentralized problem for each CAV i is formulated as follows:

$$\min_{u_i(t)} \frac{1}{2} \int_{t_i^0}^{t_i^{m^*}} u_i^2(t)\, dt, \tag{18}$$

subject to : (2), (3), (14), $p_i(t_i^0) = 0, p_i(t_i^{m^*}) = L$, and given t_i^0, v_i^0.

Observe that we have omitted the rear end safety constraint (4) and the lateral collision constraint (6). The latter applies to the MZ and affects (18) only at $t = t_i^{m^*}$ which is implicitly handled by the selection of $t_i^{m^*}$ in (14). The former, on the other hand, must be satisfied for all $t \in [t_i^0, t_i^{m^*}]$, whereas (14) only guarantees that it is satisfied at $t = t_i^{m^*}$. It is omitted here because we will show that the solution of (18) guarantees that this constraint indeed holds throughout $[t_i^0, t_i^{m^*}]$ under proper initial conditions (t_i^0, v_i^0); note that the constraint also holds in $[t_i^{m^*}, t_i^f]$ under Assumption 2.

3.1. Analytical solution of the decentralized optimal control problem

For the analytical solution of (18) and its online implementation, we apply Hamiltonian analysis under Assumption 1, i.e., when the CAVs enter the CZ none of the constraints is active. We stress that this is not in general true. For example, a CAV may enter the CZ with speed higher than the speed limit. In this case, a solution of the optimal control problem is infeasible. A feasibility analysis for CAVs to satisfy such initial conditions is discussed in Section 3.2 where we show that a feasible region $\mathcal{F}_i \subset R^2$ of initial conditions (t_i^0, v_i^0) for CAV i exists such that $s_i(t) \geqslant \delta$ for all $t \in [t_i^0, t_i^m]$; a feasibility enforcement analysis to ensure the existence of feasible and optimal solutions is given in Zhang, Cassandras et al. (2017).

From (18), the state Eqs. (2), and the control/state constraints (3), for each vehicle $i \in \mathcal{N}(t)$ the Hamiltonian function with the state and control constraints adjoined is

$$\begin{aligned} H_i\big(t, p(t), v(t), u(t)\big) &= \frac{1}{2}u_i^2 + \lambda_i^p \cdot v_i + \lambda_i^v \cdot u_i \\ &+ \mu_i^a \cdot (u_i - u_{max}) + \mu_i^b \cdot (u_{min} - u_i) + \mu_i^c \cdot (v_i - v_{max}) \\ &+ \mu_i^d \cdot (v_{min} - v_i), \end{aligned} \tag{19}$$

where λ_i^p and λ_i^v are the costates, and μ^T is a vector of Lagrange multipliers with

$$\mu_i^a = \begin{cases} > 0, & u_i(t) - u_{max} = 0, \\ = 0, & u_i(t) - u_{max} < 0, \end{cases} \tag{20}$$

$$\mu_i^b = \begin{cases} > 0, & u_{min} - u_i(t) = 0, \\ = 0, & u_{min} - u_i(t) < 0, \end{cases} \tag{21}$$

$$\mu_i^c = \begin{cases} > 0, & v_i(t) - v_{max} = 0, \\ = 0, & v_i(t) - v_{max} < 0, \end{cases} \tag{22}$$

$$\mu_i^d = \begin{cases} > 0, & v_{min} - v_i(t) = 0, \\ = 0, & v_{min} - v_i(t) < 0. \end{cases} \tag{23}$$

The Euler–Lagrange equations become

$$\dot{\lambda}_i^p = -\frac{\partial H_i}{\partial p_i} = 0, \tag{24}$$

and

$$\dot{\lambda}_i^v = -\frac{\partial H_i}{\partial v_i} = \begin{cases} -\lambda_i^p, & v_i(t) - v_{max} < 0 \text{ and} \\ & v_{min} - v_i(t) < 0, \\ -\lambda_i^p - \mu_i^c, & v_i(t) - v_{max} = 0, \\ -\lambda_i^p + \mu_i^d, & v_{min} - v_i(t) = 0, \end{cases} \tag{25}$$

with boundary conditions $p_i(t_i^0) = 0, p_i(t_i^m) = L, \lambda_i^v(t_i^m) = 0$, given initial conditions $t_i^0, v_i(t_i^0)$, and t_i^m specified by (14). The necessary condition for optimality is

$$\frac{\partial H_i}{\partial u_i} = u_i + \lambda_i^v + \mu_i^a - \mu_i^b = 0. \tag{26}$$

To address this problem, constrained and unconstrained arcs need to be pieced together to satisfy (24) through (26). Based on our state and control constraints (3) and boundary conditions, the optimal solution is the result of different combinations of the following possible arcs.

1. Control and State Constraints not Active. In this case, we have $\mu_i^a = \mu_i^b = \mu_i^c = \mu_i^d = 0$. Applying (26), the optimal control is given by

$$u_i + \lambda_i^v = 0, \quad i \in \mathcal{N}(t) \tag{27}$$

and the Euler–Lagrange equations yield (24) and

$$\dot{\lambda}_i^v = -\frac{\partial H_i}{\partial v_i} = -\lambda_i^p. \tag{28}$$

From (24) we have $\lambda_i^p = a_i$ and (28) implies $\lambda_i^v = -(a_i t + b_i)$, where a_i and b_i are integration constants. Consequently, the optimal control input (acceleration/deceleration) as a function of time is given by

$$u_i^*(t) = a_i t + b_i. \tag{29}$$

Substituting this equation into the vehicle dynamics (2) we can find the optimal speed and position for each vehicle, namely

$$v_i^*(t) = \frac{1}{2}a_i t^2 + b_i t + c_i \tag{30}$$

$$p_i^*(t) = \frac{1}{6}a_i t^3 + \frac{1}{2}b_i t^2 + c_i t + d_i, \tag{31}$$

where c_i and d_i are integration constants. These fours constants above can be computed by using the initial and final conditions in (18). In particular, using (30) with the initial condition $v_i(t_i^0) = v_i^0$, (31) with the initial and terminal conditions $p_i(t_i^0) = 0$, $p_i(t_i^m) = L$, and the boundary condition of the costate $\lambda_i^v(t_i^m) = -u_i(t_i^m) = 0$, we can form the system of four equations of the form $\mathbf{T_i b}_i = \mathbf{q}_i$:

$$\begin{bmatrix} \frac{1}{6}(t_i^0)^3 & \frac{1}{2}(t_i^0)^2 & t_i^0 & 1 \\ \frac{1}{2}(t_i^0)^2 & t_i^0 & 1 & 0 \\ \frac{1}{6}(t_i^m)^3 & \frac{1}{2}(t_i^m)^2 & t_i^m & 1 \\ -t_i^m & -1 & 0 & 0 \end{bmatrix} \cdot \begin{bmatrix} a_i \\ b_i \\ c_i \\ d_i \end{bmatrix} = \begin{bmatrix} p_i(t_i^0) \\ v_i(t_i^0) \\ p_i(t_i^m) \\ \lambda_i^v(t_i^m) \end{bmatrix} \tag{32}$$

where t_i^m is specified by (14). Note that since (32) can be computed online, the controller may re-evaluate the four constants in the form $a_i(t, p_i, v_i)$, $b_i(t, p_i, v_i)$, $c_i(t, p_i, v_i)$, and $d_i(t, p_i, v_i)$ at any time $t > t_i^0$ to get

$$\mathbf{b}_i(t, p_i(t), v_i(t)) = (\mathbf{T}_i)^{-1}.\mathbf{q}_i(t, p_i(t), v_i(t)) \tag{33}$$

and update (29) as follows

$$u_i^*(t, p_i(t), v_i(t)) = a_i(t, p_i(t), v_i(t))t + b_i(t, p_i(t), v_i(t)). \tag{34}$$

Thus, feedback can be indirectly provided through the re-calculation of the vector $\mathbf{b}_i(t, p_i(t), v_i(t))$ in (33).

2. Control Constraint Active, $u_i^*(t) = u_{max}$. Suppose that at time $t = t_1$, (29) becomes

$$u_i^*(t) = u_{max}, \ \forall t \geq t_1 \tag{35}$$

while $v_{min} < v_i(t) < v_{max}$. In this case, the Hamiltonian is continuous at $t = t_1$ (entry point of the control constrained arc). Substituting the last equation into the vehicle dynamics (2), we can find the optimal speed and position of each vehicle, namely

$$v_i^*(t) = u_{max}\, t + f_i, \tag{36}$$

$$p_i^*(t) = \frac{1}{2}u_{max}\, t^2 + f_i\, t + e_i, \ \forall t \geq t_1 \tag{37}$$

where f_i and e_i are constants of integration that can be computed easily since we know the speed and position of the vehicle at time $t = t_1$.

3. Control and State Constraints Active, $u_i(t) = u_{max}$ and $v_i(t) = v_{max}$. Suppose that at time $t = t_2 > t_1$ (exit point of the control constrained arc and entry point of the state variable constrained arc), (36) becomes $v_i^*(t) = v_{max}$. Then from (2) we have $\dot{v}_i^* = u_i^*(t) = 0$ for $t > t_2$, and the Hamiltonian is discontinuous at $t = t_2$ (entry point of the state constrained arc $v_i^*(t) = v_{max}$); see Bryson (1975). It follows from (2) that for $t \geq t_2$

$$p_i^*(t) = v_{max}\, t + r_i, \tag{38}$$

where r_i is the constant of integration that can be computed from the position of the vehicle at $t = t_2^-$.

Given certain terminal constraints, it is possible that the state variable constraint becomes inactive again; see Bryson (1975). If this happens at time $t = t_3 > t_2$ (exit point of the corner) the state variable constraint becomes inactive again, i.e., $v_{min} < v_i(t) < v_{max}$, then the Hamiltonian and costates are continuous at $t = t_3$, i.e., $H(t_3^-) = H(t_3^+)$, $\lambda_i^p(t_3^-) = \lambda_i^p(t_3^+) = g_i$, and $\lambda_i^v(t_3^-) = \lambda_i^v(t_3^+) = -(g_i t + h_i)$, where g_i and h_i are constants of integration. Hence

$$-\frac{1}{2}u_i^*(t) = g_i(v_{max} - v_i(t)). \tag{39}$$

The optimal control input, speed, and position are

$$u_i^*(t) = g_i t + h_i, \tag{40}$$

$$v_i^*(t) = \frac{1}{2}g_i t^2 + h_i t + q_i, \tag{41}$$

$$p_i^*(t) = \frac{1}{6}g_i t^3 + \frac{1}{2}h_i t^2 + q_i t + s_i, \tag{42}$$

where the constants of integration g_i, h_i, q_i, and s_i can be computed from the control, speed, and position of the vehicle at $t = t_3^-$ and (39) at $t = t_3^+$.

4. Control Constraints Active, $u_i(t) = u_{min}$. Suppose that at time $t = t_1$, (29) becomes $u_i^*(t) = u_{min}$ while $v_{min} < v_i(t) < v_{max}$. In this case, the Hamiltonian is continuous at $t = t_1$ (entry point of the control constrained arc). It follows from (2) that for $t \geq t_1$

$$v_i^*(t) = u_{min}\, t + f_i, \tag{43}$$

$$p_i^*(t) = \frac{1}{2}u_{min}\, t^2 + f_i\, t + e_i, \tag{44}$$

where f_i and e_i are constants of integration that can be computed easily since we know the speed and position of the vehicle at time $t = t_1$.

5. Control and State Constraints Active, $u_i(t) = u_{min}$ and $v_i(t) = v_{min}$. Suppose that at time $t = t_2 > t_1$ (exit point of the control constrained arc and entry point of the state variable constrained arc), (43) becomes equal to v_{min}. Then from (2) we have $\dot{v}_i^* = u_i^*(t) = 0$ for $t > t_2$, and the Hamiltonian is discontinuous at $t = t_2$ (corner). Substituting $u_i^*(t) = 0$ for $t > t_2$ into the vehicle dynamics equations (2) we can find the optimal speed and position of each vehicle for $t \geq t_2$, namely

$$p_i^*(t) = v_{min}\, t + r_i \tag{45}$$

where r_i is the constant of integration that can be computed from the position of the vehicle at $t = t_2^-$.

If at time $t = t_3 > t_2$ (exit point of the corner) the state variable constraint becomes inactive again, i.e., $v_{min} < v_i(t) < v_{max}$, then the Hamiltonian and costates are continuous at $t = t_3$. The analysis follows the discussion at the exit point of the corner in the case where $u_i(t) = u_{max}$ and $v_i(t) = v_{max}$, and the optimal control input, speed, and position are given by (40)–(42).

6. State Constraints Active, $v_i(t) = v_{max}$. Suppose that at time $t = t_1$, (30) becomes $v_i^*(t) = v_{max}$ while $u_{min} < u_i(t) < u_{max}$. Then from (2) we have $\dot{v}_i^* = u_i^*(t) = 0$ for $t > t_1$, and the Hamiltonian is discontinuous at $t = t_1$. Substituting $u_i^*(t) = 0$ into the vehicle

dynamics equations (2) we can also find the optimal position of each vehicle for $t \geq t_1$, namely

$$p_i^*(t) = v_{max}\, t + r_i \tag{46}$$

where r_i is the constant of integration that can be computed from the position of the vehicle at $t = t_1^-$.

If at time $t = t_3 > t_2$ (exit point of the state constrained arc) the state variable constraint becomes inactive again, i.e., $v_{min} < v_i(t) < v_{max}$, then the Hamiltonian and costates are continuous at $t = t_3$. The analysis follows the discussion at the exit point of the state constrained arc in the case where $u_i(t) = u_{max}$ and $v_i(t) = v_{max}$, and the optimal control input, speed, and position are given by (40)–(42).

7. State Constraints Active, $v_i(t) = v_{min}$. Suppose that at time $t = t_1$, (30) becomes $v_i^*(t) = v_{min}$ (entry point of the state variable constrained arc) while $u_{min} < u_i(t) < u_{max}$. Then from (2) we have $\dot{v}_i^* = u_i^*(t) = 0$ for $t > t_1$, and the Hamiltonian is discontinuous at $t = t_1$. It follows from (2) that for $t \geq t_1$

$$p_i^*(t) = v_{min}\, t + r_i \tag{47}$$

where r_i is the constant of integration that can be computed from the position of the vehicle at $t = t_1^-$. The analysis is similar to the case where $u_i(t) = u_{max}$ and $v_i(t) = v_{max}$, and the optimal control input, speed, and position are given by (40)–(42).

To derive the analytical solution of (18), we follow the standard methodology used in optimal control problems with interior point state and/or control constraints. Namely, we first start with the unconstrained arc and derive the solution using (32). If the solution violates any of the state or control constraints, then the unconstrained arc is pieced together with the arc corresponding to the violated constraint, and we re-solve the problem with the two arcs pieced together. The two arcs yield a set of algebraic equations which are solved simultaneously using the boundary conditions of (18) and interior conditions between the arcs. If the resulting solution, which includes the determination of the optimal switching time from one arc to the next one, violates another constraint, then the last two arcs are pieced together with the arc corresponding to the new violated constraint, and we re-solve the problem with the three arcs pieced together. The three arcs will yield a new set of algebraic equations that need to be solved simultaneously using the boundary conditions of (18) and interior conditions between the arcs. The resulting solution includes the optimal switching time from one arc to the next one. The process is repeated until the solution does not violate any other constraints.

Remark 3. The simple nature of the optimal control and states in (29) through (31) makes the online solution of (18) computationally feasible, even with the additional burden of checking for active constraints in Cases 2) through 7). However, there is an additional feature of the solution that we can exploit, i.e., the fact that the control structure for CAV i remains unchanged until an "event" e.g., unexpected braking by the preceding vehicle, rescheduling of the crossing order by the coordinator, etc.) occurs that affects its behavior. Therefore, there is no need for a time-driven controller implementation such that $u_i^*(t)$ is repeatedly re-evaluated. Rather, an event-driven controller may be used without affecting its optimality properties under conditions such as those described in Zhong and Cassandras (2010).

3.2. Feasibility analysis for safety constraints

As already pointed out, the decentralized problem (18) does not explicitly include the safety constraints (4) and (6). While the latter holds by the construction of t_i^m in (14) and is needed only over $[t_i^m, t_i^f]$, the former is not guaranteed to hold for all $t \in [t_i^0, t_i^m]$.

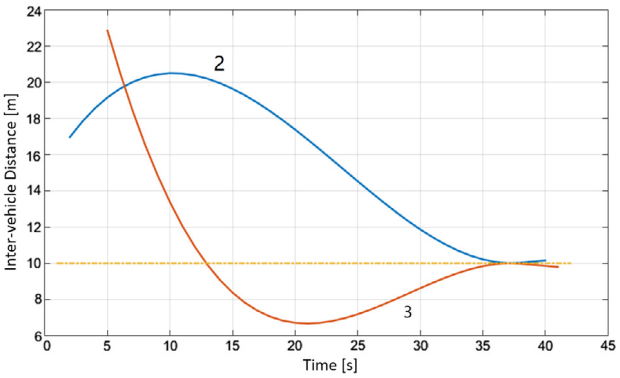

Fig. 2. Example of safety constraint violation by CAV 3 when $\delta = 10$.

We begin with a simple example of how (4) may be violated under the optimal control (29). This is illustrated in Fig. 2 with $\delta = 10$ for two CAVs that follow each other in the same lane within the CZ. We can see that while (4) is eventually satisfied, due to the constraints imposed on the solution of (18) through (6), the controller (29) is unable to maintain (4) throughout the CZ. What is noteworthy in Fig. 2 is that (4) is violated by CAV 3 at an interval which is *interior* to $[t_3^0, t_3^f]$, i.e., the form of the optimal control solution (29) causes this violation even though the constraint is initially satisfied at $t_3^0 = 5$ in Fig. 2.

Recall that we use k to denote the CAV physically preceding i on the same lane, and that $i-1$ is the CAV ahead of i in the queue. Clearly, $k \leqslant i-1$; when $k = i-1$, then i follows $i-1$ in the same lane, whereas if $i-1$ is on a different lane from i, then $k < i-1$. Using this notation, the following theorem asserts that we can always find initial conditions (t_i^0, v_i^0) which guarantee the safety constraint (4) holds throughout the CZ under the decentralized optimal control, even though (4) is not explicitly included in (18).

Theorem 2. *There exists a nonempty feasible region $\mathcal{F}_i \subset R^2$ of initial conditions (t_i^0, v_i^0) for CAV i such that, under the decentralized optimal control, $s_i(t) \geqslant \delta$ holds for all $t \in [t_i^0, t_i^m]$ given initial and final conditions $t_k^0, v_k^0, t_k^m, v_k^m$ for CAV k.*

Proof. See Appendix.

For any set of initial conditions which are feasible, our analysis gives an optimal control solution, possibly with a constrained arc. The case which applies depends on the choice of initial conditions. In other words, our analysis provides a map from the feasible region to a set of optimal controls for CAV i which all satisfy the safety inequality. Theorem 2 asserts that as long as we can drive the CAV to a feasible initial point, there exists a solution satisfying the safety inequality over the entire CZ and MZ which may or may not include a constrained arc. There are two possible ways to deal with the feasibility issue. One approach is to guide the CAV through an appropriately designed "Feasibility Enforcement Zone" (FEZ) that precedes the CZ and to make adjustments so as to attain a feasible initial condition when it reaches the CZ. The associated feasibility enforcement analysis and the design process of a FEZ are extensively discussed in Zhang, Cassandras et al. (2017). Alternatively, if a FEZ is not realizable and a CAV arrives with $(t_i^0, v_i^0) \notin \mathcal{F}_i$, then the decentralized nature of (18) allows us to forego its optimal control and settle for a non-optimal but safe control instead with some t_i^m which is supplied to CAV $i+1$ so as to continue the use of (29) for all subsequent CAVs.

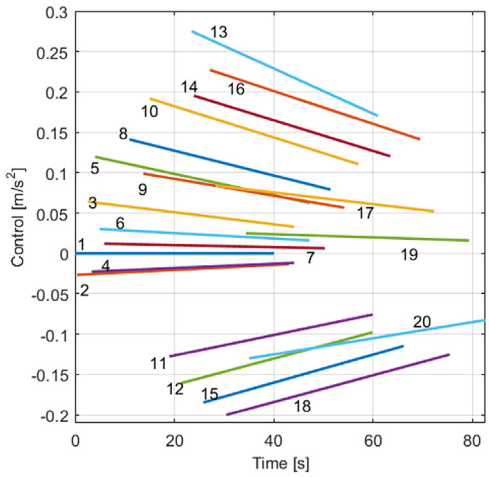

Fig. 3. Optimal control input signal of the first 20 vehicles in the queue.

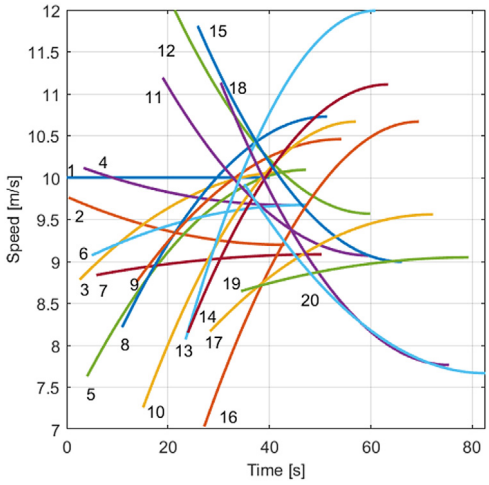

Fig. 4. Speed of the first 20 vehicles in the queue.

4. Simulation results

To evaluate the effectiveness of the proposed solution, we considered the following two case studies: (1) coordination of 20 vehicles, (2) coordination of 448 vehicles. For the first study we used MATLAB and for the second one we used VISSIM, a microscopic multi-modal traffic flow commercial simulation software package. The proposed solution was compared to a baseline scenario, where the intersection has traffic lights with fixed switching times. To quantify the impact of the vehicle coordination on fuel consumption, we used the polynomial metamodel proposed in Kamal, Mukai, Murata, and Kawabe (2013) that yields vehicle fuel consumption as a function of the speed, $v(t)$, and control input, $u(t)$.

In the first case study, we considered a single intersection, where the length of the MZ, S, is 30 m and the length of the CZ, L, is 400 m. The minimum safe distance, δ, between two vehicles was set to be 10 m. The maximum and minimum speed limits are 13 m/s and 0, respectively. The maximum acceleration limit is 0.2 m/s^2 and the maximum deceleration is set to be arbitrarily large. The control input and the optimal speed for each vehicle in the queue is shown in Figs. 3 and 4. Note that CAV # 16 violates both the control constraint $u(t) \leq u_{max}$ and the state constraint $v(t) \leq v_{max}$.

In the second case study, we considered two actual intersections in tandem located in Boston. For each direction, only one lane is considered. We set $L = 245$ m and $S = 35$ m for both intersections. As the shapes of the actual intersections are not regular, the distance between them is not the same for different directions; in particular, the distance in the lane where the traffic flow coming from the east is 160 m, whereas the distance in the lane where the traffic flow goes from the west is 145 m. In this study, we do not consider the coupling of the two intersections. The vehicle arrival rate is assumed to be given by a Poisson process with $\lambda = 450$ veh/h for each lane. A comparison to the baseline scenario using traffic lights is shown in Fig. 5. The fuel consumption improvement was 46.6%, while the travel time was improved by 30.9%. The fuel consumption improvement is due to the following reasons: (1) the vehicles do not come to a full stop, thereby conserving momentum, and (2) each vehicle travels with the minimum acceleration/deceleration inside the CZ so that transient engine operation is minimized with direct benefits in fuel consumption.

5. Concluding remarks and future work

We have addressed the problem of optimally controlling CAVs crossing an urban intersection without any explicit traffic signaling. The objective was to minimize energy consumption subject to a throughput maximization requirement and hard safety constraints. We have shown that the solution of the latter depends only on the hard safety constraints imposed on CAVs and that its structure enables a decentralized energy minimization optimal control problem formulation whose terminal time depends only on a "neighboring" set of CAVs. We presented a complete analytical solution of these decentralized problems and derived conditions under which feasible solutions satisfying all safety constraints always exist. The effectiveness of the proposed solution was validated through simulation which showed that the benefits of the proposed framework are substantial.

In our decentralized framework, we considered full penetration of identical CAVs having access to perfect information (no errors or delays). We also did not consider lane changing, turns or pedestrians. Ongoing research is considering turns [see Zhang, Malikopoulos, and Cassandras (2017)] and lane changing in the intersection with a diverse set of CAVs and exploring the associated tradeoffs between the intersection throughput and fuel consumption of each individual vehicle. Another issue that we are considering is the potential rear-end collision that would occur inside the MZ if the terminal speeds of two vehicles i and k traveling on the same lane are different. If this case arises, there are two possible approaches to adopt. The first approach is to set $v_i(t_i^m) = v_k(t_k^m)$ and solve the optimal control problem for CAV i with a specified terminal speed. Alternatively, we can simply forgo the assumption of constant speed in the MZ and ensure the absence of rear-end collision. We are also investigating the implications of the proposed approach to adjacent intersections and a feasibility enforcement to ensure that each CAV starts from a feasible state; see Zhang, Cassandras et al. (2017). The fact that the control structure for each CAV remains unchanged until an "event" occurs that affects its behavior is an additional feature of the solution that is being exploited and which will eventually lead to event-driven controllers.

The first-in-first-out queue imposes several limitations that can become even more apparent in heavy-volume traffic situations. An important direction for future research is to relax the first-in-first-out queue and establish a higher-level dynamic optimization problem the solution of which would yield online the optimal "scheduling" for the CAVs to cross the intersection. Future research should also consider different penetrations of CAVs, which can alter significantly the efficiency of the entire system, e.g., what is the

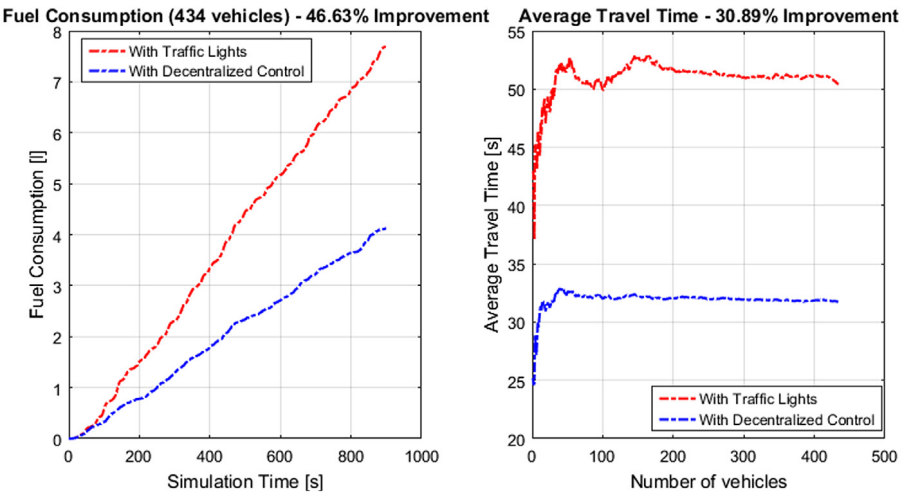

Fig. 5. Fuel consumption and average travel time improvement.

critical traffic flow rate beyond which the benefits of CAVs reach their limit? In fact, as the arrival rates increase, the optimization process may result in occasional stopping and restarting due to the implicit state constraint $v_i(t) \geq 0$. Although it is relatively straightforward to extend our results to the case where the perfect information assumption is relaxed, future research needs to be directed at the implications of errors and/or delays.

Appendix A. Proof of Lemma 1

Using the second form of the objective function in (11) and recalling that $t_1^{m^*}$ is fixed by the unconstrained control $u_1(t) \in \mathcal{U}_1$, the solution $\mathbf{t}^*$ is obtained by minimizing t_i^{m*} for every $i = 2, \ldots, N$. There are three cases to consider:

Case 1: If $i-1 \in \mathcal{R}_i(t) \cup \mathcal{O}_i(t)$, then (6) cannot become active. On the other hand, (4) may become active if there exists some $k \in \mathcal{L}_i(t)$ such that $k \in \mathcal{R}_{i-1}(t) \cup \mathcal{O}_{i-1}(t)$, thus creating an interdependence between i and $i-1$ through k. If this happens, (4) implies that $p_k(t_i^m) - p_i(t_i^m) = L + v_k^m(t_i^m - t_k^m) - L \geqslant \delta$, hence $t_i^m - t_k^m \geq \frac{\delta}{v_k^m}$. Therefore, t_i^m is minimized by setting

$$t_i^m = t_k^m + \frac{\delta}{v_k^m}. \tag{48}$$

Recalling that $t_i^m - t_{i-1}^m \geq 0$ from (1), it follows that the optimal value of t_i^m in this case is given by

$$t_i^{m^*} = \max\{t_{i-1}^{m^*}, t_k^{m^*} + \frac{\delta}{v_k^m}\}. \tag{49}$$

Case 2: If $i-1 \in \mathcal{L}_i(t)$, then (6) cannot become active, but constraint (4) can. It follows that (49) applies with $k = i-1$, yielding

$$t_i^{m^*} = t_{i-1}^{m^*} + \frac{\delta}{v_{i-1}^m}. \tag{50}$$

Case 3: If $i-1 \in \mathcal{C}_i(t)$, then constraint (6) can become active. It follows that $t_i^m \geq t_{i-1}^f = t_{i-1}^m + \frac{S}{v_{i-1}^m}$. Including the possibility that (4) becomes active if there exists some $k \in \mathcal{L}_i(t)$ such that $k \in \mathcal{R}_{i-1}(t) \cup \mathcal{O}_{i-1}(t)$, and recalling (1), we have

$$t_i^{m^*} = \max\{t_{i-1}^{m^*} + \frac{S}{v_{i-1}^m}, t_k^{m^*} + \frac{\delta}{v_k^m}\}. \tag{51}$$

Observe that if such $k \in \mathcal{L}_i(t)$ exists, then $k \in \mathcal{C}_{i-1}(t)$, since k and i are in the same lane. Therefore, $i-1$ and $k < i-1$ must also satisfy (6), i.e., $t_{i-1}^{m^*} \geq t_k^{m^*} + \frac{S}{v_k^m}$, hence $t_{i-1}^{m^*} + \frac{S}{v_{i-1}^m} \geq t_k^{m^*} + \frac{S}{v_k^m} + \frac{S}{v_{i-1}^m} > t_k^{m^*} + \frac{\delta}{v_k^m}$, since $S > \delta$. It follows that

$$t_i^{m^*} = t_{i-1}^{m^*} + \frac{S}{v_{i-1}^m}. \tag{52}$$

Combining (49), (50) and (52) we obtain (12). □

Appendix B. Proof of Theorem 1

When constraints (3) are allowed to be active in (11), then the values of t_i^m determined through Lemma 1 may not be attainable in minimizing $t_i^m - t_1^m$. Thus, we seek a lower bound to t_i^m, which is independent of these constraints. There are two cases to consider depending on t_i^0 and on whether CAV i can reach v_{max} prior to t_{i-1}^m or not:

(i) If CAV i enters the CZ at t_i^0, accelerates with u_{max} until it reaches v_{max} and then cruises at this speed until it leaves the MZ at time t_i^{1f}, it was shown in Zhang et al. (2016) that $t_i^{1f} = t_i^0 + \frac{L+S}{v_{max}} + \frac{(v_{max}-v_i^0)^2}{2u_{max}v_{max}}$. From Assumption 2, the time it reaches the MZ is $t_i^{1f} - \frac{S}{v_{max}} = t_i^1$ in (15).

(ii) If CAV i accelerates with u_{max} but reaches the MZ at t_i^m with speed $v_i(t_i^m) < v_{max}$, it was shown in Zhang et al. (2016) that it leaves the MZ at time $t_i^{2f} = t_i^0 + \frac{v_i(t_i^m)-v_i^0}{u_{max}} + \frac{S}{v_i(t_i^m)}$ where $v_i(t_i^m) = \sqrt{2Lu_{i,max} + (v_i^0)^2}$. From Assumption 2, the time it reaches the MZ is $t_i^{2f} - \frac{S}{v_i(t_i^m)} = t_i^2$ in (16).

Thus, $t_i^c = t_i^1 \mathbb{1}_{v_i^m = v_{max}} + t_i^2(1 - \mathbb{1}_{v_i^m = v_{max}})$ ($\mathbb{1}$ is the indicator function) is a lower bound of t_i^f regardless of the solution of (11). Combining this lower bound with Lemma 1, we immediately obtain (14) including $t_1^{m^*}$ which is a free variable dependent on $\mathscr{A}_1$. □

Appendix C. Proof of Theorem 2

To prove the existence of the feasible region, there are two cases to consider, depending on whether any state or control constraint for either CAV i or k becomes active in the CZ.

Case 1: No state or control constraint is active for either k or i over $[t_i^0, t_i^m]$. By using (31), (32) and the definition $s_i(t) = p_k(t) -$

$p_i(t)$, under optimal control we can write

$$\begin{aligned} s_i(t; t_i^0, v_i^0) &= s_i(t, t_i^m, v_i^m, t_k^0, v_k^0, t_k^m, v_k^m; t_i^0, v_i^0) \\ &= A(t, t_i^m, v_i^m, t_k^0, v_k^0, t_k^m, v_k^m; t_i^0, v_i^0)t^3 \\ &\quad + B(t, t_i^m, v_i^m, t_k^0, v_k^0, t_k^m, v_k^m; t_i^0, v_i^0)t^2 \\ &\quad + C(t, t_i^m, v_i^m, t_k^0, v_k^0, t_k^m, v_k^m; t_i^0, v_i^0)t \\ &\quad + D(t, t_i^m, v_i^m, t_k^0, v_k^0, t_k^m, v_k^m; t_i^0, v_i^0), \end{aligned} \tag{53}$$

where A, B, C and D are functions defined over $t \in [t_i^0, t_i^m]$. Recall that CAV k is cruising in the MZ, so that (29) through (31) do not apply for k over $[t_k^m, t_i^m]$ leading to different expressions for A, B, C and D. Therefore, we consider two further subcases, one for $[t_i^0, t_k^m]$ and the other for $[t_k^m, t_i^m]$. For ease of notation, in the sequel we replace (t_i^0, v_i^0) by (τ, υ).

Case 1.1: $t \in [t_i^0, t_k^m]$. In this case, $s_i(t; \tau, \upsilon)$ is a cubic polynomial inheriting the cubic structure of (31). We can solve (32) for the coefficients a_k, b_k, c_k, d_k, a_i, b_i, c_i and d_i using the initial and final conditions of CAVs k and i. Then, denoting A, B, C and D as $A_1(\tau, \upsilon)$, $B_1(\tau, \upsilon)$, $C_1(\tau, \upsilon)$ and $D_1(\tau, \upsilon)$ for $t \in [t_i^0, t_k^m]$, these are explicitly given by

$$\begin{aligned} A_1(\tau, \upsilon) &= \frac{1}{(t_k^0 - t_k^m)^3}(2L + (v_k^m + v_k^0)(t_k^0 - t_k^m)) \\ &\quad - \frac{1}{(\tau - t_i^m)^3}(2L + (v_i^m + \upsilon)(\tau - t_i^m)), \\ B_1(\tau, \upsilon) &= -\frac{1}{(t_k^0 - t_k^m)^3}[3L(t_k^0 + t_k^m) \\ &\quad + (v_k^0(t_k^0 + 2t_k^m) + v_k^m(2t_k^0 + t_k^m))(t_k^0 - t_k^m)] \\ &\quad + \frac{1}{(\tau - t_i^m)^3}[3L(\tau + t_i^m) \\ &\quad + (\upsilon(\tau + 2t_i^m) + v_i^m(2\tau + t_i^m))(\tau - t_i^m)], \\ C_1(\tau, \upsilon) &= \frac{1}{(t_k^0 - t_k^m)^3}[6t_k^0 t_k^m L + [(v_k^0((t_k^m)^2 + 2t_k^0 t_k^m) \\ &\quad + v_k^m((t_k^0)^2 + 2t_k^m t_k^0))](t_k^0 - t_k^m)] \\ &\quad - \frac{1}{(\tau - t_i^m)^3}[6\tau t_i^m L + [(\upsilon((t_i^m)^2 + 2\tau t_i^m) \\ &\quad + v_i^m((\tau)^2 + 2t_i^m \tau))](\tau - t_i^m)], \\ D_1(\tau, \upsilon) &= \frac{1}{(t_k^0 - t_k^m)^3}[L((t_k^0)^3 - 3(t_k^0)^2 t_k^m) \\ &\quad - (v_k^0 t_k^0 (t_k^m)^2 + v_k^m (t_k^0)^2 t_k^m)(t_k^0 - t_k^m)] \\ &\quad - \frac{1}{(\tau - t_i^m)^3}[L((\tau)^3 - 3(\tau)^2 t_i^m) \\ &\quad - (\upsilon\tau(t_i^m)^2 + v_i^m(\tau)^2 t_i^m)(\tau - t_i^m)]. \end{aligned} \tag{54}$$

Note that in (53) we write $s_i(t; \tau, \upsilon)$ (recall that $(t_i^0, v_i^0) \equiv (\tau, \upsilon)$) to emphasize the dependence of $s_i(t)$ on these initial conditions for CAV i, i.e., we give a parametric characterization of $s_i(t)$ through (τ, υ). Aside from (τ, υ), the function $s_i(t)$ also depends on two groups of arguments: (*i*) t_k^0, v_k^0, t_k^m and $v_k^m \equiv v_k(t_k^f) = v_k(t_k^m)$ are quantities associated with CAV k. Since $k < i$, all information related to this CAV is available and is fixed throughout $[t_i^0, t_i^m]$. (*ii*) t_i^m and $v_i^m \equiv v_i(t_i^f) = v_i(t_i^m)$ are quantities which can also be determined through CAV k or $i-1$.

To summarize, $s_i(t; \tau, \upsilon)$ varies only with t and (τ, υ) with all remaining arguments being known to CAV i. First, observing that the first half of each of the coefficient expressions in (54) (which is derived by solving (31) and (32) for CAV k) is a constant fully determined by information provided by CAV k, we can rewrite these as $K_{A_1}, K_{B_1}, K_{C_1}, K_{D_1}$. Therefore, $p_k^*(t)$ in (31) can be expressed as

$$p_k^*(t) = K_{A_1} t^3 + K_{B_1} t^2 + K_{C_1} t + K_{D_1}. \tag{55}$$

Next, the second half of the coefficients can be expressed through polynomials in either τ or υ explicitly derived by solving (31) and (32) for CAV i. We will use the notation $P_{X,n}(\tau)$, $P_{X,n}(\upsilon)$ to represent polynomials of degree $n = 1, 2, 3$ and $X \in \{A_1, B_1, C_1, D_1\}$. Similarly, we set $Q_3(\tau) = (\tau - t_i^m)^3$. Thus, for the coefficients in Eq. (54), we get

$$\begin{aligned} A_1(\tau, \upsilon) &= K_{A_1} + \frac{P_{A_1,1}(\tau)P_{A_1,1}(\upsilon)}{Q_3(\tau)}, \\ B_1(\tau, \upsilon) &= K_{B_1} + \frac{P_{B_1,2}(\tau)P_{B_1,1}(\upsilon)}{Q_3(\tau)}, \\ C_1(\tau, \upsilon) &= K_{C_1} + \frac{P_{C_1,3}(\tau) + P_{C_1,2}(\tau)P_{C_1,1}(\upsilon)}{Q_3(\tau)}, \\ D_1(\tau, \upsilon) &= K_{D_1} + \frac{P_{D_1,3}(\tau) + P_{D_1,2}(\tau)P_{D_1,1}(\upsilon)}{Q_3(\tau)}. \end{aligned} \tag{56}$$

Note that $p_k^*(t)$ in (55) involves only the K terms, while the analogous cubic polynomial for $p_i^*(t)$ involves only the P and Q terms.

Our goal is to ensure that $s_i(t; \tau, \upsilon) \geqslant \delta$ for all $t \in [\tau, t_k^m]$ (recall that $t_i^0 \equiv \tau$). We can guarantee this by ensuring that $s_i^*(\tau, \upsilon) \equiv \min_{t \in [\tau, t_k^m]}\{s_i(t; \tau, \upsilon)\} \geqslant \delta$. Thus, we shift our attention to the determination of $s_i^*(\tau, \upsilon)$. We can obtain expressions for the first and the second derivative of $s_i(t; \tau, \upsilon)$, $\dot{s}_i(t; \tau, \upsilon)$ and $\ddot{s}_i(t; \tau, \upsilon)$ respectively, from (53), as follows:

$$\begin{aligned} \dot{s}_i(t; \tau, \upsilon) &= v_k(t) - v_i(t) = 3A_1(\tau, \upsilon)t^2 + 2B_1(\tau, \upsilon)t \\ &\quad + C_1(\tau, \upsilon), \end{aligned} \tag{57}$$

$$\ddot{s}_i(t; \tau, \upsilon) = u_k(t) - u_i(t) = 6A_1(\tau, \upsilon)t + 2B_1(\tau, \upsilon). \tag{58}$$

Clearly, we can determine $t_i^* \equiv \arg\min_{t \in [\tau, t_k^m]}\{s_i(t; \tau, \upsilon)\}$ as the solution of $\dot{s}_i(t; \tau, \upsilon) = 0$ with $\ddot{s}_i(t; \tau, \upsilon) \geqslant 0$, unless $s_i^*(\tau, \upsilon)$ occurs at the boundaries, i.e., $t_i^* = \tau$ or $t_i^* = t_k^m$. Thus, there are three cases to consider:

Case 1.1.A: $t_i^* = \tau$. In this case,

$$\begin{aligned} s_i^*(\tau, \upsilon) &= s_i(\tau; \tau, \upsilon) \\ &= A_1(\tau, \upsilon)\tau^3 + B_1(\tau, \upsilon)\tau^2 + C_1(\tau, \upsilon)\tau + D_1(\tau, \upsilon) \geqslant \delta \end{aligned} \tag{59}$$

and we can satisfy $s_i(\tau, \upsilon) \geqslant \delta$ for any υ as long as a feasible τ is determined. Since at $t = \tau$, we have $p_i(\tau) = 0$ and using the definition of $s_i(t) = p_k(t) - p_i(t)$ and (55), we get

$$s_i(\tau) = p_k^*(\tau) = K_{A_1}\tau^3 + K_{B_1}\tau^2 + K_{C_1}\tau + K_{D_1}.$$

Observe that if

$$p_k(\tau) \geqslant \delta$$

then CAV i enters the CZ at a safe distance from its preceding CAV k and since $t_i^* = \tau$, we have $s_i(t; \tau, \upsilon) \geqslant \delta$ for all $t \in [\tau, t_k^m]$. Thus, it suffices to select $\tau \geqslant t_k^\delta$, where t_k^δ is the smallest real root of $p_k(\tau) - \delta = 0$.

Case 1.1.B: $t_i^* = t_k^m$. In this case,

$$\begin{aligned} s_i^*(\tau, \upsilon) &= s_i(t_k^m; \tau, \upsilon) \\ &= A_1(\tau, \upsilon)(t_k^m)^3 + B_1(\tau, \upsilon)(t_k^m)^2 + C_1(\tau, \upsilon)t_k^m \\ &\quad + D_1(\tau, \upsilon) \geqslant \delta. \end{aligned} \tag{60}$$

Thus, the feasibility region $\mathcal{F}_i$ is defined by all (τ, υ) such that $s_i(t_k^m; \tau, \upsilon) - \delta \geq 0$ in the (τ, υ) space.

Case 1.1.C: $t_i^* = t_1 \in (\tau, t_k^m)$. This case only arises if the discriminant $\mathcal{D}_i(\tau, \upsilon)$ of (57) is positive, i.e.,

$$\mathcal{D}_i(\tau, \upsilon) = 4B_1(\tau, \upsilon)^2 - 12A_1(\tau, \upsilon)C_1(\tau, \upsilon) > 0 \tag{61}$$

and we get

$$t_1 = \frac{-2B_1(\tau,\upsilon) \pm \sqrt{\mathcal{D}_i(\tau,\upsilon)}}{6A_1(\tau,\upsilon)}. \tag{62}$$

In addition, we must have

$$\tau < t_1 < t_k^m, \;\; \dot{s}_i(t_1;\tau,\upsilon) = 0, \;\; \ddot{s}_i(t_1;\tau,\upsilon) \geqslant 0. \tag{63}$$

Therefore, the feasibility region $\mathcal{F}_i$ is defined by all (τ,υ) such that

$$\begin{aligned} s_i^*(\tau,\upsilon) &= s_i(t_1;\tau,\upsilon) \\ &= A_1(\tau,\upsilon)(t_1)^3 + B_1(\tau,\upsilon)(t_1)^2 + C_1(\tau,\upsilon)t_1 \\ &\quad + D_1(\tau,\upsilon) \geqslant \delta \end{aligned} \tag{64}$$

in conjunction with (62)–(63).

Case 1.2: $t \in (t_k^m, t_i^m]$. Over this interval, $v_k(t) = v_k^m$ by Assumption 2. Therefore, (29)–(31) no longer apply: (29) becomes $u_k^*(t) = 0$, (30) becomes $v_k^*(t) = v_k^m$ and (31) becomes $p_k^*(t) = L + v_k^m(t - t_k^m)$. Evaluating $s_i(t) = p_k(t) - p_i(t)$ in this case yields the following coefficients in (54):

$$\begin{aligned} A_2(\tau,\upsilon) &= -\frac{1}{(\tau - t_i^m)^3}(2L + (v_i^m + \upsilon)(\tau - t_i^m)), \\ B_2(\tau,\upsilon) &= \frac{1}{(\tau - t_i^m)^3}[3L(\tau + t_i^m) + (\upsilon(\tau + 2t_i^m) \\ &\quad + v_i^m(2\tau + t_i^m))(\tau - t_i^m)], \\ C_2(\tau,\upsilon) &= v_k^m - \frac{1}{(\tau - t_i^m)^3}[6\tau t_i^m L + [(\upsilon((t_i^m)^2 + 2\tau t_i^m) \\ &\quad + v_i^m((\tau)^2 + 2t_i^m\tau))](\tau - t_i^m)], \\ D_2(\tau,\upsilon) &= L - v_k^m t_k^m - \frac{1}{(\tau - t_i^m)^3}[L((\tau)^3 - 3(\tau)^2 t_i^m) \\ &\quad - (\upsilon\tau(t_i^m)^2 + v_i^m(\tau)^2 t_i^m)(\tau - t_i^m)]. \end{aligned} \tag{65}$$

It follows that $K_{A_1}, K_{B_1}, K_{C_1}$ and K_{D_1} in (56) should be modified accordingly, giving $K_{A_2} = K_{B_2} = 0$, $K_{C_2} = v_k^m$ and $K_{D_2} = L - v_k^m t_k^m$. Since we are assuming that no control or state constraints are active for CAV i, the designated final time t_i^m under optimal control satisfies (12), i.e., $s_i(t_i^m) \geq \delta$. Thus, we only need to consider the subcase where $s_i^*(\tau,\upsilon)$ occurs in (t_k^m, t_i^m) and we have

$$t_i^* = t_2, \quad t_2 \in (t_k^m, t_i^m).$$

Proceeding as in *Case 1.1.C*, the feasibility region $\mathcal{F}_i$ is defined by all (τ,υ) such that

$$\begin{aligned} s_i^*(\tau,\upsilon) &= s_i(t_2;\tau,\upsilon) \\ &= A_2(\tau,\upsilon)(t_2)^3 + B_2(\tau,\upsilon)(t_2)^2 + C_2(\tau,\upsilon)t_2 \\ &\quad + D_2(\tau,\upsilon) \geqslant \delta \end{aligned} \tag{66}$$

in conjunction with (62)–(63), with A_1, B_1, C_1 and D_1 replaced by A_2, B_2, C_2 and D_2, and with $\tau < t_1 < t_k^m$ replaced by $t_k^m < t_2 < t_i^m$.

Case 2: At least one of the state and control constraints is active over $[\tau, t_i^m]$. As discussed in Section 3.1, there are several cases to consider when state and/or control constraints are active. Since one or both CAVs k and i may experience an active constraint, all different combinations need to be considered. We analyze a few in what follows since it is clear that the remaining cases are handled in a similar fashion.

Case 2.1: $v_k^*(t) = v_{max}$ over an optimal trajectory arc, while CAV i is unconstrained. In this case, (29)–(31) no longer apply for CAV k and the coefficients in (54) are affected similar to *Case 1.2*, except that the fixed speed v_k^m is now v_{max}.

First, consider the interval $[\tau, t_k^m]$. Following the Hamiltonian analysis in Section 3.1, let t_k^I be the time CAV k enters the constrained arc with $v_k^*(t) = v_{max}$ and t_k^E be the time it exits this arc (see subfigure (a) in Fig. 6). The trajectory of CAV k consists of three arcs as follows. First, for $t \in [\tau, t_k^I]$, A_1, B_1, C_1 and D_1 are defined exactly as in (54). Second, for $t \in [t_k^I, t_k^E]$, (29)–(31) are replaced by $u_k^*(t) = 0$, and $v_k^*(t) = v_{max}$ and (31) becomes $p_k^*(t) = p_k(t_k^I) + v_{max}(t - t_k^I)$, where $p_k(t_k^I)$ can be determined before CAV i enters the CZ. The form of the coefficients in (54) is modified the same way as in (65), with v_k^m and L replaced by v_{max} and $p_k(t_k^I)$. It follows that $K_{A_1}, K_{B_1}, K_{C_1}$ and K_{D_1} in (56) should also be modified accordingly, with $K_{A_2} = K_{B_2} = 0$, $K_{C_2} = v_{max}$ and $K_{D_2} = p_k(t_k^I) - v_{max}t_k^I$. The final arc is for $t \in [t_k^E, t_k^m]$, when CAV k returns to an unconstrained arc. The form of the coefficients in (54) does not change, except that A_1, B_1, C_1 and D_1 should be replaced by A_3, B_3, C_3 and D_3 since the value of the coefficients may differ for different unconstrained arcs.

As in *Case 1.1*, we next consider $t_i^* \equiv \arg\min_{t\in[\tau,t_k^m]}\{s_i(t;\tau,\upsilon)\}$ and there are three cases.

Case 2.1.A: $t_i^* = \tau$. As in *Case 1.1.A*, it suffices to select $\tau \geqslant t_k^\delta$ where t_k^δ is the smallest real root of $p_k^*(\tau) = \delta$.

Case 2.1.B: $t_i^* = t_k^m$. As in *Case 1.1.B*, the feasibility region $\mathcal{F}_i$ is defined by all (τ,υ) such that $s_i(t_k^m;\tau,\upsilon) - \delta \geq 0$ in the (τ,υ) space, with A_1, B_1, C_1 and D_1 being replaced by A_3, B_3, C_3 and D_3.

Case 2.1.C: $t_i^* = t_1 \in (\tau, t_k^m)$. This case may only arise for $t \in (\tau, t_k^I)$. As in *Case 1.1.C*, the feasibility region $\mathcal{F}_i$ is defined by

$$\begin{aligned} s_i^*(\tau,\upsilon) &= s_i(t_1;\tau,\upsilon) \\ &= A_1(\tau,\upsilon)(t_1)^3 + B_1(\tau,\upsilon)(t_1)^2 + C_1(\tau,\upsilon)t_1 \\ &\quad + D_1(\tau,\upsilon) \geqslant \delta \end{aligned} \tag{67}$$

in conjunction with (62)–(63) with $\tau < t_1 < t_k^m$ being replaced by $\tau < t_1 < t_k^I$.

For $t \in (t_k^m, t_i^m]$, the analysis is exactly the same as the way we handle *Case 1.2*, with A_2, B_2, C_2 and D_2 being replaced by A_4, B_4, C_4 and D_4. The feasibility region $\mathcal{F}_i$ is defined by

$$\begin{aligned} s_i^*(\tau,\upsilon) &= s_i(t_2;\tau,\upsilon) \\ &= A_4(\tau,\upsilon)(t_2)^3 + B_4(\tau,\upsilon)(t_2)^2 + C_4(\tau,\upsilon)t_2 \\ &\quad + D_4(\tau,\upsilon) \geqslant \delta \end{aligned} \tag{68}$$

in conjunction with (62)–(63).

Case 2.2: CAV k is unconstrained and $u_i^*(t) = u_{min}$ over an optimal trajectory arc. Since there are many subcases and each can be similarly handled, we only consider one subcase where CAV i enters the constrained arc at t_k^m (see subfigure (b) in Fig. 6).

Since both CAV k and i are unconstrained in $[\tau, t_k^m]$, the form of the coefficients in (54) does not change, and the feasibility region for *Cases 2.2.A, 2.2.B* and *2.2.C* can be derived in the same way as *Case 1.1.A, 1.1.B* and *1.1.C*. For $t \in (t_k^m, t_i^m]$, CAV i is decelerating at a constant value $u_i^*(t) = u_{min}$. Thus, (29)–(31) are replaced by $u_i^*(t) = u_{min}$, $v_i^*(t) = v_i(t_k^m) + u_{min}(t - t_k^m)$ and $p_i^*(t) = L + v_i(t)(t - t_k^m)$, where $v_i(t_k^m)$ can be determined given (τ,υ). The coefficients in (54) are modified as follows:

$$\begin{aligned} A_2(\tau,\upsilon) &= 0, \\ B_2(\tau,\upsilon) &= -\frac{1}{2}u_{min}, \\ C_2(\tau,\upsilon) &= v_k^m - v_i(t_k^m) + u_{min}t_k^m, \\ D_2(\tau,\upsilon) &= -v_k^m t_k^m. \end{aligned} \tag{69}$$

For $t \in (t_k^m, t_i^m]$, CAV k is cruising at the speed v_k^m and CAV i keeps decelerating until it reaches v_i^m. Therefore, s_i^* may only occur at t_i^m and we have

$$\begin{aligned} s_i^*(\tau,\upsilon) &= s_i(t_i^m;\tau,\upsilon) \\ &= A_2(\tau,\upsilon)(t_i^m)^3 + B_2(\tau,\upsilon)(t_i^m)^2 + C_2(\tau,\upsilon)t_i^m \\ &\quad + D_2(\tau,\upsilon) \geqslant \delta. \end{aligned} \tag{70}$$

Thus, the feasibility region $\mathcal{F}_i$ is defined by all (τ,υ) such that $s_i(t_i^m;\tau,\upsilon) - \delta \geq 0$ in the (τ,υ) space.

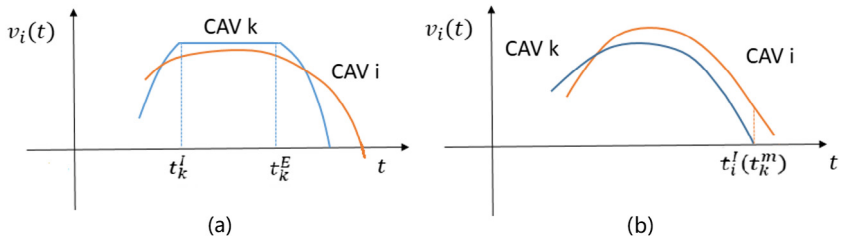

Fig. 6. Cases when the state and/or control constraints are active.

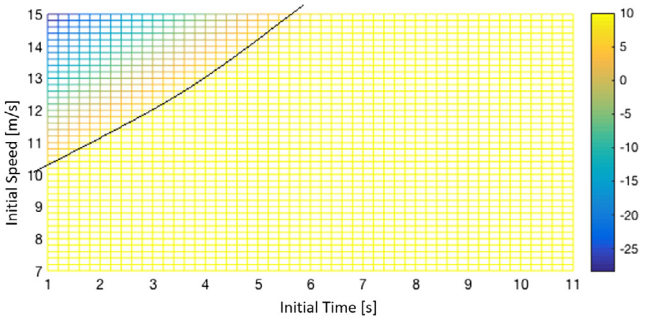

Fig. 7. Feasible and infeasible region. (For interpretation of the references to color in this figure legend, the reader is referred to the web version of this article.)

All remaining cases are similarly handled and in each case a feasibility region $\mathcal{F}_i$ is defined by all (τ, υ) satisfying an inequality of the form $s_i(\sigma; \tau, \upsilon) - \delta \geq 0$ for an appropriate value of σ and coefficients in (53).

To complete the proof, we show that feasibility region $\mathcal{F}_i$ is always nonempty. This is easily established by considering a point (τ, υ) such that $v_{pmin} < \upsilon < v_{max}$ (which is possible by Assumption 1) and $\tau = t_k^f$: since $p_k^*(t_k^f) = L + S$ and $p_i^*(\tau) = 0$, it follows that $s_i(\tau) > S > \delta$. Obviously, any such (τ, υ) is feasible. □

Remark 4. To illustrate the feasible region and provide some intuition, we give a numerical example (see Fig. 7), with $\delta = 10$, $L = 400$, and CAV k is the first vehicle in the CZ and is driving at the constant speed $v_k^0 = v_k^m = 10$. The color bar in Fig. 7 indicates the value of $s_i^*(t)$ and the yellow region, determined by (64), represents the feasible region, while the non-yellow region represents the infeasible region. The black curve is the boundary between the two regions and is not linear in general. This boundary curve shifts depending on the different cases we have considered in the proof of Theorem 2. This example also illustrates that we can always find a nonempty feasible region since we can select points to the right of the curve corresponding to CAV i entry times in the CZ which can be arbitrarily large.

References

Alonso, J., Milanés, V., Pérez, J., Onieva, E., González, C., & de Pedro, T. (2011). Autonomous vehicle control systems for safe crossroads. *Transportation Research Part C: Emerging Technologies*, *19*(6), 1095–1110.

Athans, M. (1969). A unified approach to the vehicle-merging problem. *Transportation Research*, (ISSN: 00411647) *3*(1), 123–133. http://dx.doi.org/10.1016/0041-1647(69)90109-9.

Bryson, A. E. (1975). *Applied optimal control: optimization, estimation and control*. CRC Press.

Colombo, A., & Del Vecchio, D. (2014). Least restrictive supervisors for intersection collision avoidance: A scheduling approach. *IEEE Transactions on Automatic Control, Provisiona*.

de La Fortelle, A. (2010). Analysis of reservation algorithms for cooperative planning at intersections. In *13th international ieee conference on intelligent transportation systems* (pp. 445–449), Sept.

Dresner, K., & Stone, P. (2004). Multiagent traffic management: a reservation-based intersection control mechanism. In *Proceedings of the third international joint conference on autonomous agents and multiagents systems* (pp. 530–537).

Dresner, K., & Stone, P. (2008). A multiagent approach to autonomous intersection management. *Journal of Artificial Intelligence Research*, *31*, 591–653.

Huang, S., Sadek, A., & Zhao, Y. (2012). Assessing the mobility and environmental benefits of reservation-based intelligent intersections using an integrated simulator. *IEEE Transactions on Intelligent Transportation Systems*, *13*(3), 1201,1214. http://dx.doi.org/10.1109/TITS.2012.2186442.

Kamal, M., Mukai, M., Murata, J., & Kawabe, T. (2013). Model predictive control of vehicles on urban roads for improved fuel economy. *IEEE Transactions on Control Systems Technology*, *21*(3), 831–841. http://dx.doi.org/10.1109/TCST.2012.2198478.

Kim, K.-D., & Kumar, P. (2014). An MPC-based approach to provable system-wide safety and liveness of autonomous ground traffic. *IEEE Transactions on Automatic Control*, *59*(12), 3341–3356. http://dx.doi.org/10.1109/TAC.2014.2351911.

Lee, J., Park, B. B., Malakorn, K., & So, J. J. (2013). Sustainability assessments of cooperative vehicle intersection control at an urban corridor. *Transportation Research Part C: Emerging Technologies*, *32*, 193–206.

Levine, W., & Athans, M. (1966). On the optimal error regulation of a string of moving vehicles. *IEEE Transactions on Automatic Control*, (ISSN: 0018-9286) *11*(3), 355–361. http://dx.doi.org/10.1109/TAC.1966.1098376.

Malikopoulos, A. A. (2011). *Real-time, Self-learning identification and stochastic optimal control of advanced powertrain systems*. ProQuest.

Malikopoulos, A. A. (2013). Stochastic optimal control for series hybrid electric vehicles. In *American Control Conference (ACC), 2013* (pp. 1189–1194). IEEE.

Malikopoulos, A. A., & Aguilar, J. P. (2013). An optimization framework for driver feedback systems. *IEEE Transactions on Intelligent Transportation Systems*, *14*(2), 955–964. http://dx.doi.org/10.1109/TITS.2013.2248058.

Margiotta, R., & Snyder, D. (2011). An agency guide on how to establish localized congestion mitigation programs. Technical report, U.S. Department of Transportation. Federal Highway Administration.

Miculescu, D., & Karaman, S. (2014). Polling-systems-based control of high-performance provably-safe autonomous intersections. In *53rd IEEE conference on decision and control*.

Ntousakis, I. A., Nikolos, I. K., & Papageorgiou, M. (2016). Optimal vehicle trajectory planning in the context of cooperative merging on highways. *Transportation Research Part C: Emerging Technologies*, *71*, 464–488.

Rajamani, R. (2012). *Vehicle dynamics and control*. Springer.

Rajamani, R., Tan, H.-S., Law, B. K., & Zhang, W.-B. (2000). Demonstration of integrated longitudinal and lateral control for the operation of automated vehicles in platoons. *IEEE Transactions on Control Systems Technology*, *8*(4), 695–708.

Rios-Torres, J., & Malikopoulos, A. A. (2017a). A survey on the coordination of connected and automated vehicles at intersections and merging at highway on-ramps. *IEEE Transactions on Intelligent Transportation Systems*, *18*(5), 1066–1077.

Rios-Torres, J., & Malikopoulos, A. A. (2017b). Automated and cooperative vehicle merging at highway on-ramps. *IEEE Transactions on Intelligent Transportation Systems*, *18*(4), 780–789.

Rios-Torres, J., Malikopoulos, A. A., & Pisu, P. (2015). Online optimal control of connected vehicles for efficient traffic flow at merging roads. In *2015 IEEE 18th international conference on intelligent transportation systems* (pp. 2432–2437).

Schrank, B., Eisele, B., Lomax, T., & Bak, J. (2015). 2015 Urban mobility scorecard. Technical report, Texas A& M Transportation Institute.

Shladover, S. E., Desoer, C. A., Hedrick, J. K., Tomizuka, M., Walrand, J., Zhang, W.-B., et al. (1991). Automated vehicle control developments in the PATH program. *IEEE Transactions on Vehicular Technology*, *40*(1), 114–130.

Tachet, R., Santi, P., Sobolevsky, S., Reyes-Castro, L. I., Frazzoli, E., Helbing, D., et al. (2016). Revisiting street intersections using slot-based systems. *Plos One*, *11*(3).

Varaiya, P. (1993). Smart cars on smart roads: problems of control. *IEEE Transactions on Automatic Control*, *38*(2), 195–207.

Yan, F., Dridi, M., & El Moudni, A. (2009). Autonomous vehicle sequencing algorithm at isolated intersections. In *2009 12th international IEEE conference on intelligent transportation systems* (pp. 1–6).

Zhang, Y., Cassandras, C. G., & Malikopoulos, A. A. (2017). Optimal control of connected automated vehicles at urban traffic intersections: A feasibility enforcement analysis. In *Proceedings of the 2017 American control conference* (pp. 3548–3553).

Zhang, Y., Malikopoulos, A. A., & Cassandras, C. G. (2016). Optimal control and coordination of connected and automated vehicles at urban traffic intersections. In *Proceedings of the American control conference* (pp. 6227–6232).

Zhang, Y., Malikopoulos, A. A., & Cassandras, C. G. (2017). Decentralized optimal control for connected automated vehicles at intersections including left and right turns. In *56th IEEE conference on decision and control* (pp. 4428–4433).

Zhong, M., & Cassandras, C. G. (2010). Asynchronous distributed optimization with event-driven communication. *IEEE Transactions on Automatic Control*, *55*(12), 2735–2750.

Zhu, F., & Ukkusuri, S. V. (2015). A linear programming formulation for autonomous intersection control within a dynamic traffic assignment and connected vehicle environment. *Transportation Research Part C: Emerging Technologies*, (ISSN: 0968090X) . http://dx.doi.org/10.1016/j.trc.2015.01.006.

Zohdy, I. H., Kamalanathsharma, R. K., & Rakha, H. (2012). Intersection management for autonomous vehicles using iCACC. In *2012 15th international IEEE conference on intelligent transportation systems* (pp. 1109–1114).

Andreas A. Malikopoulos is an Associate Professor in the Department of Mechanical Engineering at the University of Delaware (UD). Before joining UD, he was the Deputy Director and the Lead of the Sustainable Mobility Theme of the Urban Dynamics Institute at Oak Ridge National Laboratory (ORNL), and a Senior Researcher with General Motors Global Research & Development. He received a Diploma from the National Technical University of Athens, Greece, in 2000, and his M.S. and Ph.D. degrees from the University of Michigan, Ann Arbor, in 2004 and 2008, respectively all in Mechanical Engineering. His research interests span several fields, including analysis, optimization, and control of cyber–physical systems; decentralized stochastic systems; stochastic scheduling and resource allocation; and complex systems. The emphasis is on applications related to energy, transportation and operations research. Dr. Malikopoulos is the recipient of several prizes and awards, including the 2007 Dare to Dream Opportunity Grant from the University of Michigan Ross School of Business, the 2007 University of Michigan Teaching Fellow, and the 2010 Alvin M. Weinberg Fellowship. He has been selected by the National Academy of Engineering to participate at the 2010 German–American Frontiers of Engineering (FOE) Symposium and organize a session in transportation at the 2016 European–American FOE Symposium. He has also been selected as a 2012 Kavli Frontiers of Science Scholar by the National Academy of Sciences. Dr. Malikopoulos is currently an Associate Editor of the IEEE Transactions on Intelligent Vehicles and IEEE Transactions on Intelligent Transportation Systems. He is a Senior Member of the IEEE and a Fellow of the ASME.

Christos G. Cassandras is Distinguished Professor of Engineering at Boston University. He is Head of the Division of Systems Engineering, Professor of Electrical and Computer Engineering, and co-founder of Boston University's Center for Information and Systems Engineering (CISE). He received degrees from Yale University (B.S., 1977), Stanford University (M.S.E.E., 1978), and Harvard University (S.M., 1979; Ph.D., 1982). In 1982–84 he was with ITP Boston, Inc. where he worked on the design of automated manufacturing systems. In 1984–1996 he was a faculty member at the Department of Electrical and Computer Engineering, University of Massachusetts/Amherst. He specializes in the areas of discrete event and hybrid systems, cooperative control, stochastic optimization, and computer simulation, with applications to computer and sensor networks, manufacturing systems, and transportation systems. He has published over 400 refereed papers in these areas, and six books. He has guest-edited several technical journal issues and currently serves on several journal Editorial Boards, including Editor of *Automatica*. In addition to his academic activities, he has worked extensively with industrial organizations on various systems integration projects and the development of decision-support software. He has most recently collaborated with The MathWorks, Inc. in the development of the discrete event and hybrid system simulator SimEvents.

Dr. Cassandras was Editor-in-Chief of the *IEEE Transactions on Automatic Control* from 1998 through 2009 and has also served as Editor for Technical Notes and Correspondence and Associate Editor. He was the 2012 President of the IEEE Control Systems Society (CSS). He has also served as Vice President for Publications and on the Board of Governors of the CSS, as well as on several IEEE committees, and has chaired several conferences. He has been a plenary/keynote speaker at numerous international conferences, including the *American Control Conference* in 2001, the *IEEE Conference on Decision and Control* in 2002 and 2016, and the 2017 *IFAC World Congress*, and has also been an IEEE Distinguished Lecturer.

He is the recipient of several awards, including the 2011 IEEE Control Systems Technology Award, the Distinguished Member Award of the IEEE Control Systems Society (2006), the 1999 Harold Chestnut Prize (IFAC Best Control Engineering Textbook) for *Discrete Event Systems: Modeling and Performance Analysis*, a 2011 prize and a 2014 prize for the IBM/IEEE Smarter Planet Challenge competition (for a "Smart Parking" system and for the analytical engine of the Street Bump system respectively), the 2014 Engineering Distinguished Scholar Award at Boston University, several honorary professorships, a 1991 Lilly Fellowship and a 2012 Kern Fellowship. He is a member of Phi Beta Kappa and Tau Beta Pi. He is also a Fellow of the IEEE and a Fellow of the IFAC.

Yue J. Zhang received the B.S. degree in electronics and information engineering from Huazhong University of Science and Technology, Wuhan, China in 2013. She is currently pursuing the Ph.D. degree with the Division of Systems Engineering and the Center for Information and Systems Engineering (CISE) at Boston University, working with Prof. Christos G. Cassandras. Her research interests include control and optimization of hybrid systems and big data analytics with applications to intelligent transportation systems. During the summer of 2015, she is working as a research intern with the National Transportation Research Center at the Oak Ridge National Laboratory.